

Evaluation of Multidisciplinary Optimization Techniques Applied to a Reusable Launch Vehicle

Nichols F. Brown*

Northrop Grumman Corporation, Fairfax, Virginia 22033

and

John R. Olds†

Georgia Institute of Technology, Atlanta, Georgia 30332

DOI: 10.2514/1.16577

Three multilevel multidisciplinary optimization techniques, Bi-Level Integrated System Synthesis, Collaborative Optimization, and Modified Collaborative Optimization, are applied to the design of a reusable launch vehicle, evaluated, and compared in this study. In addition to comparing the techniques against each other, they are also compared with designs reached via fixed-point iteration of disciplines with local optimization and the industry accepted multidisciplinary optimization technique, All-at-Once. The new multidisciplinary optimization techniques, particularly Bi-Level Integrated System Synthesis, showed greater ability than fixed-point iteration to design for a global objective and were more applicable to complex systems than All-at-Once. This study was the first time that the novel multidisciplinary optimization methods were compared qualitatively and quantitatively under controlled experimentation practices. It is still impossible to statistically determine whether any one of the novel multidisciplinary optimization techniques is better than another, because more studies using different test problems corroborating the conclusions made here are needed.

Nomenclature

A	=	area
c^*	=	characteristic exhaust velocity
c_F	=	thrust coefficient
g	=	inequality constraint
h	=	equality constraint/enthalpy/altitude
I_{sp}	=	specific impulse
\dot{m}	=	mass rate
MR	=	mass ratio, $W_{gross}/W_{insertion}$
P	=	power
p	=	pressure
$Perf$	=	performance
$Prop$	=	propulsion
r	=	fuel to oxidizer mixture ratio (propellant mixture ratio)
S	=	wing area
SF	=	scale factor
T	=	thrust
W	=	weight
w	=	weighting factor (for BLISS)
$W\&S$	=	weights and sizing
X	=	input or design variable
Y	=	output or behavior variable
ΔV	=	change in velocity
ε	=	nozzle expansion ratio
θ	=	pitch angle rate
Φ	=	design objective

Subscripts

c	=	combustor
e	=	exit
eng	=	engine
loc	=	local
o	=	optimized
ref	=	reference
req	=	required
sh	=	shared input to multiple CAs but not calculated by any CA (for BLISS)
SL	=	sea-level
sys	=	system
t	=	throat
vac	=	vacuum
veh	=	vehicle

Superscripts

pf	=	performance (for CO and MCO)
pp	=	propulsion (for CO and MCO)
t	=	target from system optimizer (for CO and MCO)
ws	=	weights and sizing (for CO and MCO)
$*$	=	output passed to a CA (for BLISS)
\wedge	=	output from a CA to system (for BLISS)

I. Introduction

OPTIMIZATION of complex engineering systems is an integral part of design. Originally, those that created aerospace vehicles were responsible for every aspect, from wing shape to propulsion. As the size of aerospace systems grew, however, the design of such enormously complex problems was broken down into disciplines concentrating only on part of the whole. Whereas breaking apart the overall problem into different contributing analyses (CAs) made it possible to design more complex systems, the ability for all designers to see how their specific changes would affect the whole was lost.

Over the years, two main design approaches have persisted. First, designers try several alternate designs and use the fixed-point iteration (FPI) process to converge them. A global criterion is used to choose the best design, but because no global optimization takes place, there is no guarantee that the global optimum is reached.

Presented as Paper 707 at the 43rd AIAA Aerospace Sciences Meeting and Exhibit, Reno Nevada, 10–13 January 2005; received 14 March 2005; revision received 2 February 2006; accepted for publication 3 February 2006. Copyright © 2006 by the American Institute of Aeronautics and Astronautics, Inc. All rights reserved. Copies of this paper may be made for personal or internal use, on condition that the copier pay the \$10.00 per-copy fee to the Copyright Clearance Center, Inc., 222 Rosewood Drive, Danvers, MA 01923; include the code \$10.00 in correspondence with the CCC.

*Systems Engineer, Mission Systems, 12900 Federal Systems Park Drive. Member AIAA.

†Associate Professor, Space Systems Design Laboratory, School of Aerospace Engineering, 270 Ferst Street. Associate Fellow AIAA.

Alternatively, All-at-Once (AAO) is a multidisciplinary design optimization (MDO) technique that will find a globally optimized system, but the technique works by having one system-level optimizer control the entire design, usually an impossibly complex task.

New multilevel MDO techniques [of which Collaborative Optimization (CO) [1], its derivative, Modified Collaborative Optimization (MCO) [2], and Bi-Level Integrated System Synthesis (BLISS), which has multiple derivatives, most notably BLISS-2000 [4], are three of the most likely to be practicable in large, real-world applications] are attempting to overcome some of these deficiencies. The work presented intends to add some insight as to which of the most novel techniques, CO, MCO, or BLISS, shows the most promise when applied to a realistic reusable launch vehicle (RLV) test problem.

II. Objectives

This study explores three main objectives:

- 1) Determine the benefits of MDO versus trying multiple design configurations converged using FPI.
- 2) Create a realistic test problem that will add to a growing field of research trying to evaluate novel MDO techniques CO, MCO, and BLISS.
- 3) Allow for across-the-board comparison of the MDO techniques by using the statistical method of blocking to remove external variability.

A. Benefits of MDO vs FPI

The arguments in favor of using FPI to test a limited number of configurations versus applying an MDO process are practical in nature. FPI has been the method of choice in the aerospace industry and most tools and practices were developed for it. Changing this FPI work structure would require a large initial investment, new training, and time to gain full acceptance. For the application of any MDO method to be worthwhile, it must show improvement in the global objective or produce project time savings offsetting its initial application cost.

B. Authenticity of Test Problem

The test problem chosen, the optimization of a next-generation RLV, should contribute to a growing body of work attempting to evaluate CO, MCO, and BLISS [5–12]. These MDO techniques were “crafted” as opposed to “rigorously derived” and lack a widely accepted mathematical proof showing for which MDO problems they are suited. Thus, the algorithms require that they be validated via a statistically significant number of test cases of realistic, complex system applications.

It is intended that the AAO method be used to validate the newer, unproven MDO techniques. This limits test problems to those that can still be handled by AAO.

C. Comparison Between CO, MCO, and BLISS

Because of statistical reasons, it is difficult to draw any conclusions between CO, MCO, and BLISS using the current literature available [5–12]:

- 1) Differences in the level of success with which each MDO technique has been applied can be attributed to external variances.
- 2) There are few comparison studies providing data points with which to draw any statistically significant conclusions.

To mitigate external variance (such as those caused by comparing techniques applied on different optimization problems, by different developers, or with different tools), this study will use the statistical practice of “blocking” [13]. Blocking helps eliminate variation due to “blocking variables,” in this case developer capacity and test problem difficulty. Blocking is achieved in this study by having a consistent developer apply all MDO techniques, by applying all to the same test problem, and by using a consistent set of computational tools. Whereas this study attempts to consistently apply all the MDO techniques evaluated in this study to mitigate external variance as

much as possible, one cannot completely remove all external variance. Other factors, such as a developer’s bias or familiarity with a particular MDO technique, time constraints due to outside schedules, etc., may still unwittingly introduce external variance. The authors are not aware of other possible external factors that may have introduced significant variance or skewed the results evaluated in this study.

Whereas this study will not settle the question of which is better, CO, MCO, or BLISS, as it is but one data point (see preceding item 2), it is one of the very first attempts at addressing the external variance problem when trying to compare the benefit, validity, and implementation cost of the new multilevel MDO techniques.

III. RLV Test Problem

Whereas a test problem is needed on which to apply the novel MDO techniques, for the goals of this study, it is not of critical issue which problem was selected, as long as it resembles one that may be used in “real world” applications.

The test problem selected is the optimization of a next-generation, single-stage-to-orbit (SSTO), earth-to-orbit RLV. Launching from the Kennedy Space Center, it delivers a 25 klb payload (~70% of the space shuttle’s payload capability [14]) to the International Space Station (ISS) (orbiting at 220 n mile \times 220 n mile \times 51.6 deg inclination). A base vehicle configuration, ACRE-92, was optimized via the use of three disciplines: propulsion, performance, and weights and sizing.

The ACRE-92 RLV [15] (Fig. 1) is a highly reusable space transportation class SSTO vehicle. It is based upon a concept dubbed WB-003 single stage shuttle [16]. Employing five liquid oxygen/liquid hydrogen (LOX/LH2) main engines, the RLV enters ISS insertion orbit (50 n mile \times 100 n mile \times 51.6 deg) and then uses the orbital maneuvering system (OMS) to raise the orbit to ISS orbit.

IV. Computational Tools

This section describes the legacy codes and other computational tools used for all technique applications.

A. Propulsion Tool

Rocket engine design tool for optimal performance (REDTOP) [17] allows for quick analysis of propulsion systems and is suitable for conceptual-level design.

REDTOP models the engine by determining the chemical reactions occurring in the combustion chamber and analyzing the expansion of hot gases traveling through a convergent-divergent nozzle. Combustion is modeled adiabatically and at constant pressure. Additional accuracy is reached through a built-in engine efficiency database.

A high-fidelity estimate of engine thrust to weight (T/W_{eng}) for the propulsion system is not provided by REDTOP, but is required for estimating the vehicle weight. Therefore, a low-fidelity estimate was

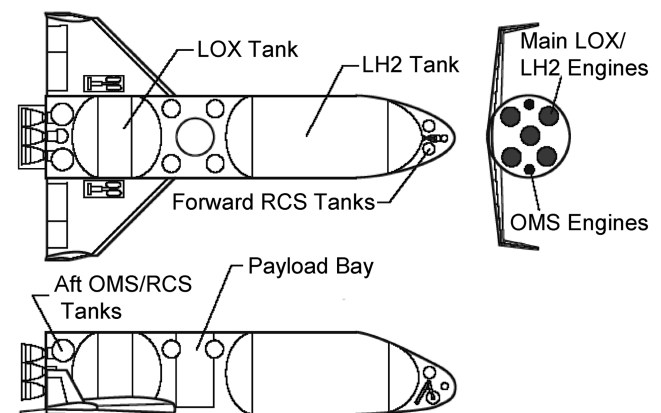


Fig. 1 Vehicle configuration, ACRE-92.

calculated based on historical data of rocket engine power to weight ratio (P/W) [18]. This calculation is as follows:

$$P = \dot{m}(h_c - h_e) \quad (1)$$

$$W_{\text{eng}} = P/k \quad (2)$$

$$T/W_{\text{eng}} = T_{\text{SL}}/W_{\text{eng}} \quad (3)$$

The sizing parameter, k , has a historical average value of $k = 520$ Btu/s/lbf based on data from 28 engines [18]. A value of $k = 600$ Btu/s/lbf was used for this study, representing the use of advanced technologies in engines for a next-generation RLV.

B. Performance Tool

Originally developed in 1970, the program to optimize simulated trajectories (POST) [19] is one of the most commonly used codes for trajectory analysis and optimization. It is a multiphase simulation program that numerically integrates the equations of motion and provides the capability to target and optimize point mass trajectories for generalized vehicles and planets.

Whereas newer versions of POST can calculate 6-degree-of-freedom (DOF) trajectories, for this project a 3-DOF simulation was executed.

C. Weights and Sizing Tool

Weights and sizing analysis is performed via a set of space shuttle derived mass estimating relationships (MERs).[‡] MERs are calculated using a spreadsheet created for this project. The MERs represent technology levels commensurate with the space shuttle; thus, technology reduction factors were implemented to represent advancements in next-generation RLVs.

D. Computational Framework

ModelCenter [20] software was used to communicate between tools. ModelCenter is a framework integration and design optimization package.

Framework integration is performed via a discipline wrapper that automatically sends inputs, executes the CA, and retrieves outputs. Discipline codes can be written in any language. In this study, REDTOP was in JAVA, POST in FORTRAN, and weights and sizing was a Microsoft Excel workbook.

Optimization is available using the design optimization tools (DOT) optimizer. DOT can perform gradient-based optimization via direct (sequential linear programming, sequential quadratic programming, and method of feasible directions) and unconstrained methods (variable metric and conjugate gradient) [21].

E. Response Surface Modeling Tool

ProbWorks [22] software package, specifically its response surface equation (RSE) generator, was used to create response surface models (RSMs) of the discipline codes when explicitly called for by an MDO technique. The RSE generator automatically creates a design of experiments (DOE) given a number of design variables and produces a wrapper containing the RSEs.

V. Fixed-Point Iteration

Fixed-point iteration or the iterative procedure [21] is the traditional way of solving a multidisciplinary analysis (MDA) problem. It is *not*, however, an MDO technique. In FPI, each discipline optimizes its part of the entire system with respect to a local variable; for example, the structures group may try maximizing strength whereas aerodynamics tries to reduce drag. FPI uses iteration to converge the system composed of multiple locally optimized disciplines, but no global system-level optimization is

executed. It is expected that FPI will provide suboptimal system-level solutions, as it does not exploit multidiscipline interactions. The customer for a system design does not care about discipline-level goals but is interested in global metrics relating to cost or weight of the entire system.

A. FPI: Formal Problem Statement

The application of FPI was unique in this study in that eight different models, each providing a converged vehicle solution, were created. The different models were a result of 1) allowing mixture ratio (r) to be controlled by propulsion (Option 1) or by weights and sizing (Option 2), 2) the local-level objective for the propulsion discipline (Φ_{Prop}) was allowed to be either Isp_{vac} or $T_{\text{SL}}/W_{\text{eng}}$, and 3) two different design spaces were applied to the design variables for the propulsion analysis.

The two propulsion design spaces evaluated were

1) Expert Design Space: Side constraints are determined by a propulsion expert as practiced in industry.

2) Large Design Space: Side constraints are maximized to not limit optimization of the system to preconceived notions.

The eight different FPI formulations investigated for this study are summarized in Table 1.

The resulting configuration with the lowest W_{dry} was selected as the best FPI configuration. Each MDO technique implementation was initialized using the best FPI configuration.

1. FPI: Propulsion Standard Form

Minimize:

$$\Phi_{\text{Prop}} = \text{Isp}_{\text{vac}} \quad \text{or} \quad - (T_{\text{SL}}/W_{\text{eng}}) \quad (4)$$

Subject to:

$$g \quad p_e \geq 5 \text{ psia} \quad (4a)$$

$$h \quad T_{\text{SL,avail}} = T_{\text{SL,req}} \quad (4b)$$

$$\text{Side} \quad 4 \leq r \leq 10 \quad \text{or} \quad 5 \leq r \leq 7$$

$$30 \leq \varepsilon \leq 100 \quad \text{or} \quad 50 \leq \varepsilon \leq 90$$

$$200 \leq p_c \leq 3100 \text{ psia} \quad \text{or} \quad 1500 \leq p_c \leq 3100 \text{ psia} \quad (4c)$$

By Changing:

$$X_{\text{loc}} \quad \varepsilon, p_c, A_t, r \quad (r \text{ only for Option 1}) \quad (4e)$$

2. FPI: Performance Standard Form

Minimize:

$$\Phi_{\text{Perf}} \quad \text{MR}_{\text{req}} \quad (5)$$

Table 1 FPI formulations investigated

Local-level objective	Mixture ratio (r) controller	Option	Design space
$\Phi_{\text{Prop}} = T_{\text{SL}}/W_{\text{eng}}$	Propulsion	1	Expert
$\Phi_{\text{Prop}} = \text{Isp}_{\text{vac}}$	Propulsion	1	Expert
$\Phi_{\text{Prop}} = T_{\text{SL}}/W_{\text{eng}}$	Propulsion	1	Large
$\Phi_{\text{Prop}} = \text{Isp}_{\text{vac}}$	Propulsion	1	Large
$\Phi_{\text{Prop}} = T_{\text{SL}}/W_{\text{eng}}$	Performance	2	Expert
$\Phi_{\text{Prop}} = \text{Isp}_{\text{vac}}$	Performance	2	Expert
$\Phi_{\text{Prop}} = T_{\text{SL}}/W_{\text{eng}}$	Performance	2	Large
$\Phi_{\text{Prop}} = \text{Isp}_{\text{vac}}$	Performance	2	Large

[‡]Personal communication: T. Talay's class notes, "ME250 Launch Vehicle Design," George Washington University, 1992.

Subject to:

$$h \quad h_{\text{insertion}} = 303,805 \text{ ft}$$

$$i_{\text{insertion}} = 51.6 \text{ deg}$$

$$\gamma_{\text{insertion}} = 0 \text{ deg} \quad (5a)$$

By Changing:

$$X_{\text{loc}} \quad \dot{\theta}_{\text{Azimuth}}, \dot{\theta}_{\text{Pitch1}}, \dot{\theta}_{\text{Pitch2}}, \dot{\theta}_{\text{Pitch3}}, \dot{\theta}_{\text{Pitch4}} \quad (5b)$$

3. FPI: Weights and Sizing Standard Form

Minimize:

$$\Phi_{W\&S} \quad W_{\text{dry}} \quad (6)$$

Subject to:

$$h \quad MR_{\text{avail}} = MR_{\text{req}} \quad (6a)$$

$$\text{Side} \quad T_{\text{SL}}/W_{\text{gross}} \geq 1.2 \quad (6b)$$

By Changing:

$$X_{\text{loc}} \quad SF_{\text{veh}}, T_{\text{SL}}/W_{\text{gross}}, r \quad (r \text{ only for Option 2}) \quad (6c)$$

B. FPI: Data Flow

To better understand the coupling of shared variables, design structure matrices (DSMs) for FPI Option 1 (Fig. 2) and Option 2 (Fig. 3) are provided. Note that a CA with local optimization is depicted with a diagonal line.

C. FPI: Results

Final configuration results for RLVs converged using the FPI method for both Option 1 and Option 2 are shown in Tables 2 and 3. Of the eight different FPI models generated, the best solution (Option 2, expert design space, $\Phi_{\text{Prop}} = \text{Isp}_{\text{vac}}$) is converged at $W_{\text{dry}} \approx 317$ klb. The best solution, however, was not the industry standard practice (Option 1, expert design space, $\Phi_{\text{Prop}} = \text{Isp}_{\text{vac}}$),

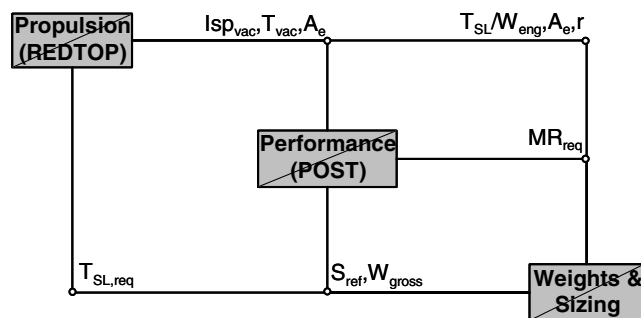


Fig. 2 DSM for FPI Option 1.

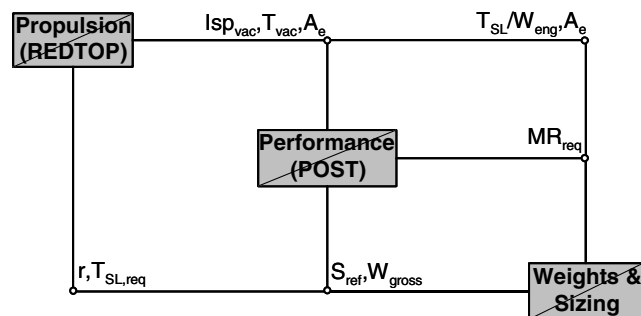


Fig. 3 DSM for FPI Option 2.

Table 2 Final configuration table for FPI Option 1^a

	Expert design space		Large design space		Units
Propulsion objective	T/W_e	Isp_{vac}	T/W_e	Isp_{vac}	—
Direction	Maximize	Maximize	Maximize	Maximize	—
$T_{\text{SL}}/W_{\text{eng}}$	60.12	58.91	73.79	58.98	—
Isp_{vac}	441.5	446.2	387.4	447.3	s
c^*	7,418	7,603	6,650	7,769	ft/s
Isp_{SL}	386.8	390.2	358.0	394.4	s
Cf_{vac}	1.874	1.856	1.816	1.824	—
Cf_{SL}	1.642	1.623	1.678	1.614	—
$T_{\text{SL}}/W_{\text{gross}}$	1.20	1.20	1.20	1.20	—
ε	50.0	50.0	30.0	46.2	—
r	7.00	6.20	10.00	5.43	—
p_c	3,100.0	3,100.0	3,100.0	3,100.0	psia
p_e	5.557	4.997	11.12	5.002	psia
A_e	261.36	286.54	431.07	319.79	ft ²
A_r	5.23	5.73	14.37	6.92	ft ²
SF	1.102	1.155	—	1.258	—
MR	8.01	7.85	10.34	7.79	—
S_{ref}	4,853	5,341	8,718	6,328	ft ²
W_{gross}	3,262,594	3,520,165	9,258,826	4,203,727	lbf
W_{dry}	320,811	356,515	714,903	433,967	lbf

^aBOLD values represent active constraints.

Table 3 Final configuration table for FPI Option 2^a

	Expert design space		Large design space		Units
Propulsion objective	T/W_e	Isp_{vac}	T/W_e	Isp_{vac}	—
Direction	Maximize	Maximize	Maximize	Maximize	—
$T_{\text{SL}}/W_{\text{eng}}$	60.12	59.06	73.56	65.32	—
Isp_{vac}	441.5	443.1	387.3	399.8	s
c^*	7,418	7,418	6,646	6,650	ft/s
Isp_{SL}	386.8	383.8	356.7	345.0	s
Cf_{vac}	1.874	1.884	1.816	1.894	—
Cf_{SL}	1.642	1.631	1.673	1.635	—
$T_{\text{SL}}/W_{\text{gross}}$	1.20	1.20	1.31	1.20	—
ε	50.0	54.3	30.0	55.9	—
r	7.00	7.00	10.00	10.00	—
p_c	3,100.0	3,100.0	2,973.5	3,100.0	psia
p_e	5.557	5.003	10.68	5.000	psia
A_e	261.38	281.56	517.20	621.07	ft ²
A_r	5.23	5.19	17.24	11.10	ft ²
SF	1.102	1.096	1.500	1.335	—
MR	8.01	7.96	10.14	9.78	—
S_{ref}	4,854	4,801	8,994	7,132	ft ²
W_{gross}	3,262,698	3,212,690	9,723,742	6,892,809	lbf
W_{dry}	320,820	317,606	769,786	560,975	lbf

^aBOLD values represent active constraints.

which converged at $W_{\text{dry}} \approx 356$ klb. Thus, it can be surmised that, when using FPI, alternating which discipline has ownership of critical shared variables can significantly affect the best resulting design converged.

VI. All-at-Once

All-at-Once is the most basic MDO technique and has wide industry acceptance, but is generally restricted to small design problems. In AAO, control is given to a system-level optimizer that ensures a global objective is met by having a single designer control the entire system.

AAO solves the global MDO problem by moving all local-level design variables and constraints away from each discipline to a new system-level optimizer entrusted with optimizing a global objective. The discipline CAs remain, but are stripped of all design responsibilities and assigned solely with analysis. The system-level

optimizer will vary all design variables and pass inputs to each discipline so that they can perform local-level disciplinary analysis.

AAO with optimizer based decomposition breaks the feedback loops between CAs in a DSM. Thus, whenever the system makes a change in the vehicle configuration, each discipline needs to run once as opposed to iterating in a tight loop, as is often true in FPI.

Whereas AAO is the most straightforward way to solve an MDO problem, it has drawbacks that make it inapplicable or impractical to the detailed design of aerospace systems. First, it takes design responsibilities away from discipline experts. Second, the design of an aerospace system is too complex for a single user or system-level optimizer to handle. Whereas AAO may solve the MDO problem for conceptual-level design, it does not scale well with complexity and is not used during detailed design.

Despite limitations, if a convex MDO problem can be solved via AAO, there is a high degree of confidence that the final configuration produced will be the true global optimum. The RLV problem presented in this paper was previously shown to be convex with a single global optimum by Cormier et al. [9]. The resultant AAO configuration will be used to validate solutions produced by applying CO, MCO, and BLISS.

A. AAO: Formal Problem Statement

AAO does not have any local-level optimization, thus the MDO problem is strictly a system-level problem.

AAO: System Standard Form

Minimize:

$$\Phi_{\text{sys}} \quad W_{\text{dry}} \quad (7)$$

Subject to:

$$\begin{aligned} g \quad p_e &\geq 5 \text{ psia} \\ T_{\text{SL}}/W_{\text{gross}} &\geq 1.2 \end{aligned} \quad (7a)$$

$$h \quad \gamma_{\text{insertion}} = 0 \text{ deg}$$

$$i_{\text{insertion}} = 51.6 \text{ deg}$$

$$h_{\text{insertion}} = 303,805 \text{ ft}$$

$$MR_{\text{req}} = MR_{\text{avail}}$$

$$S_{\text{ref,guess}} = S_{\text{ref,actual}}$$

$$W_{\text{gross,actual}} = W_{\text{gross,guess}}$$

$$T_{\text{SL,avail}} = T_{\text{SL,req}} \quad (7b)$$

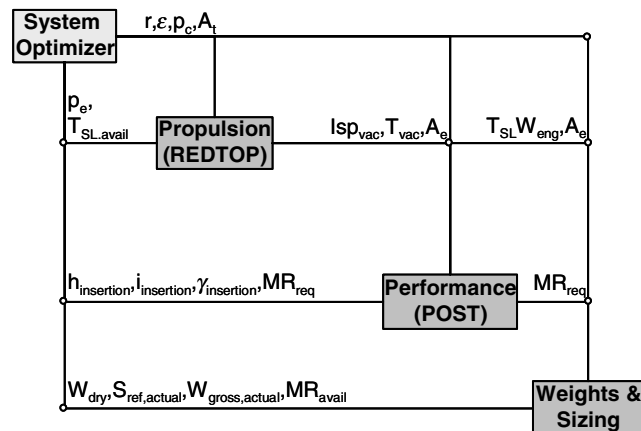


Fig. 4 DSM for AAO.

Table 4 Final configuration table for AAO^a

	AAO, full	AAO, reduced	Units
System objective	W_{dry}	W_{dry}	—
Direction	Minimize	Minimize	—
$T_{\text{SL}}/W_{\text{eng}}$	59.76	59.27	—
Isp_{vac}	439.6	440.1	s
c^*	7,291	7,282	ft/s
Isp_{SL}	380.3	378.4	s
Cf_{vac}	1.896	1.902	—
Cf_{SL}	1.641	1.635	—
$T_{\text{SL}}/W_{\text{gross}}$	1.207	1.200	—
ε	55.2	57.5	—
r	7.47	7.51	—
p_c	3,099.9	3,100.0	psia
p_e	5.243	4.999	psia
A_e	279.84	290.13	ft ²
A_t	5.07	5.05	ft ²
SF	1.076	1.073	—
MR	8.06	8.07	—
S_{ref}	4,629	4,610	ft ²
W_{gross}	3,149,989	3,138,648	lbf
W_{dry}	306,413	305,101	lbf

^aBOLD values represent active constraints.

$$\begin{aligned} \text{Side} \quad 40.29 &\leq \dot{\theta}_{\text{Azimuth}} \leq 44.53 \text{ deg/s} \\ &-1.533 \leq \dot{\theta}_{\text{Pitch1}} \leq -1.386 \text{ deg/s} \\ 0.04191 &\leq \dot{\theta}_{\text{Pitch2}} \leq 0.0543 \text{ deg/s} \\ &-0.2696 \leq \dot{\theta}_{\text{Pitch3}} \leq -0.2440 \text{ deg/s} \\ &-0.1421 \leq \dot{\theta}_{\text{Pitch4}} \leq -0.1285 \text{ deg/s} \\ 6.3 &\leq r \leq 7.7 \\ 45 &\leq \varepsilon \leq 60 \\ 4.705 &\leq A_t \leq 5.750 \text{ ft}^2 \\ 2790 &\leq p_c \leq 3100 \text{ psia} \\ 0.9913 &\leq SF \leq 1.21169 \\ 1.2 &\leq T_{\text{SL}}/W_{\text{gross}} \leq 1.5 \\ 4368 &\leq S_{\text{ref,guess}} \leq 5339 \text{ ft}^2 \\ 2936 &\leq W_{\text{gross,guess}} \leq 3559 \text{ klb} \end{aligned} \quad (7c)$$

By Changing:

$$\begin{aligned} X_{\text{sys}} \quad &\dot{\theta}_{\text{Azimuth}}, \dot{\theta}_{\text{Pitch1}}, \dot{\theta}_{\text{Pitch2}}, \dot{\theta}_{\text{Pitch3}}, \dot{\theta}_{\text{Pitch4}}, r, \varepsilon, A_t, \\ &p_c, SF, T_{\text{SL}}/W_{\text{gross}}, S_{\text{ref,guess}}, W_{\text{gross,guess}} \end{aligned} \quad (7d)$$

B. AAO: Data Flow

The DSM for AAO is shown in Fig. 4.

C. AAO: Results

Scalability difficulty was encountered during the course of this study when the system optimizer tried to simultaneously optimize all vehicle design variables.

One can observe in Table 4 that when “AAO, full” was used, $T_{\text{SL}}/W_{\text{gross}}$ seemed to approach its constrained minimum (1.2) while p_c approached its constrained maximum (3100 psia). However, the optimizer was unable to reach the constrained limits. This is common in engineering models where legacy tools have significant numerical error, making it difficult to determine derivatives necessary for gradient optimization. This can be helped by reducing the number of design variables in the system optimizer. When the values of $T_{\text{SL}}/W_{\text{gross}}$ and p_c are manually set as parameters at the constrained limits, the optimizer has an easier time reaching the true optimum solution for the test problem, “AAO, reduced.”

AAO produced a 3.94% reduction in W_{dry} versus the best FPI model and a 2.30% reduction in W_{gross} .

VII. Bi-Level Integrated System Synthesis

Bi-Level Integrated System Synthesis was originally developed by Sobieszczanski-Sobieski et al. The first version of BLISS [3] was developed in 1998 with the most recent derivative, BLISS-2000 [4], introduced in 2002. BLISS-2000 was applied in this study as it was designed as an improvement on the original BLISS based on the evaluation of several BLISS variants [12].

BLISS intends to solve large MDO problems, while at the same time minimizing the number of changes needed by current design practices. BLISS, like CO and MCO, uses a two-level MDO model (with both local and system-level optimization) to emulate the conventional organizational structure used in industry. It also lets experts have most of the control over local discipline design, thus taking advantage of expert knowledge. Because it does not add new local design variables, CAs can be performed similarly to current practices developed for use in an FPI process.

To coordinate between disciplines, BLISS uses weighting factors on local outputs to produce an overall system-level MDO solution. The system optimizer handles shared inputs or coupling variables and new weighting factors, used to dynamically control each discipline's local-level objective. With the addition of new variables, which have the potential to complicate system-level optimization, it is expected that BLISS, like CO and MCO, is best suited for MDO problems with low dimensionality coupling.

A feature of BLISS-2000 is the creation of RSMs of all CAs and applying the bi-level optimization scheme directly to the RSMs instead of the original legacy tools. Substituting for the original codes is intended to avoid the numerical integration and stability problems often associated with legacy tools. RSMs provide optimizers with smoother numerical gradients and save execution time.

RSMs require the original CAs run a DOE to create the data for fitting the RSMs. This could be a costly endeavor if there are many local-level design variables. On the other hand, using parallel execution to distribute this process over a computer network means that, in theory, this could be done in the time required to execute the most time-consuming CA once. If the RSM is not an accurate fit of the original tools, then additional DOEs may be needed until the design space is small enough to bring RSE error within acceptable tolerances. A "BLISS iteration" [4] occurs when the design space is decreased around the previous configuration and new RSMs are created.

A. BLISS: Formal Problem Statement

BLISS-2000 has both system and local-level optimization.

1. BLISS: System Standard Form

Minimize:

$$\Phi_{\text{sys}} \quad W_{\text{dry}} \quad (8)$$

Subject to:

$$h \quad Y^* = Y_o^{\wedge}(X_{\text{sys}}) \quad (8a)$$

By Changing:

$$X_{\text{sys}} \quad X_{\text{sh}} \quad r \quad (8b)$$

$$Y^* \quad \text{Isp}_{\text{vac}}, T_{\text{vac}}, A_e, T_{\text{SL}}/W_{\text{eng}}, S_{\text{ref}}, W_{\text{gross}}, T_{\text{SL,req}}, \text{MR}_{\text{req}} \quad (8c)$$

$$w \quad w1[\text{Isp}_{\text{vac}}], w2[T_{\text{vac}}], w3[A_e], w4[T_{\text{SL}}/W_{\text{eng}}], w5[W_{\text{dry}}], w6[S_{\text{ref}}], w7[W_{\text{gross}}], w8[T_{\text{SL,Req}}] \quad (8d)$$

In the preceding equation, for $w1 \dots w8$ the []s show the variable to which the weighting factor corresponds.

2. BLISS: Propulsion Standard Form

Minimize:

$$\Phi_{\text{Prop}} \quad w1(\text{Isp}_{\text{vac}}) + w2(T_{\text{vac}}) + w3(A_e) + w4(T_{\text{SL}}/W_{\text{eng}}) \quad (9)$$

Subject to:

$$g \quad p_e \geq 5 \text{ psia} \quad (9a)$$

$$h \quad T_{\text{SL,avail}} = T_{\text{SL,req}} \quad (9b)$$

$$\text{Side} \quad 4 \leq r \leq 10$$

$$30 \leq \varepsilon \leq 100$$

$$200 \leq p_c \leq 3100 \text{ psia} \quad (9c)$$

Given as Parameter:

$$X_{\text{sh}} \quad r \quad (9d)$$

$$Y^* \quad T_{\text{SL,req}} \quad (9e)$$

$$w \quad w1, w2, w3, w4 \quad (9f)$$

Find:

$$Y_o^{\wedge} \quad \text{Isp}_{\text{vac}}, T_{\text{vac}}, A_e, T_{\text{SL}}/W_{\text{eng}} \quad (9g)$$

By Changing:

$$X_{\text{loc}} \quad \varepsilon, p_c, A_t \quad (9h)$$

3. BLISS: Performance Standard Form

Minimize:

$$\Phi_{\text{Perf}} \quad \text{MR}_{\text{req}} \quad (10)$$

Subject to:

$$h \quad h_{\text{insertion}} = 303,805 \text{ ft}$$

$$i_{\text{insertion}} = 51.6 \text{ deg}$$

$$\gamma_{\text{insertion}} = 0 \text{ deg} \quad (10a)$$

Given as Parameter:

$$Y^* \quad \text{Isp}_{\text{vac}}, T_{\text{vac}}, A_e, S_{\text{ref}}, W_{\text{gross}} \quad (10b)$$

Find:

$$Y_o^{\wedge} \quad \text{MR}_{\text{req}} \quad (10c)$$

By Changing:

$$X_{\text{loc}} \quad \dot{\theta}_{\text{Azimuth}}, \dot{\theta}_{\text{Pitch1}}, \dot{\theta}_{\text{Pitch2}}, \dot{\theta}_{\text{Pitch3}}, \dot{\theta}_{\text{Pitch4}} \quad (10d)$$

4. BLISS: Weights and Sizing Standard Form

Minimize:

$$\Phi_{\text{W\&S}} \quad w5(W_{\text{dry}}) + w6(S_{\text{ref}}) + w7(W_{\text{gross}}) + w8(T_{\text{SL,req}}) \quad (11)$$

Subject to:

$$h \quad \text{MR}_{\text{avail}} = \text{MR}_{\text{req}} \quad (11a)$$

$$\text{Side} \quad T_{\text{SL}}/W_{\text{gross}} \geq 1.2 \quad (11b)$$

Given as Parameter:

$$X_{\text{sh}} \quad r \quad (11c)$$

$$Y^* \quad T_{SL}/W_{eng}, A_e, MR_{req} \quad (11d)$$

$$w \quad w5, w6, w7, w8 \quad (11e)$$

Find:

$$Y_o^* \quad W_{dry}, S_{ref}, W_{gross}, T_{SL,req} \quad (11f)$$

By Changing:

$$X_{loc} \quad SF, T_{SL}/W_{gross} \quad (11g)$$

B. BLISS: Data Flow

The DSM for BLISS is shown in Fig. 5.

C. BLISS: Results

As previously mentioned, the BLISS-2000 algorithm substitutes time-consuming legacy codes with RSMs.

In Table 5, column “BLISS-2000, RSM” indicates values derived using RSMs. “BLISS-2000, actual” indicates the actual values calculated using legacy codes. Equality between the two columns indicates that RSMs accurately modeled the CAs.

For this study a second-order central composite DOE was used to create all the discipline RSMs.

Table 5 shows that the second-order polynomial RSM models were of high fidelity. The optimum W_{dry} calculated by RSMs was virtually identical to the actual value output by the CAs.

Furthermore, the system optimal (W_{dry}) value derived by BLISS-2000 was very close to that derived by AAO. Thus, BLISS was able to find the global optimum and produced a 3.76% reduction in W_{dry} versus the best FPI result and a 2.75% reduction in W_{gross} .

VIII. Collaborative Optimization

Collaborative Optimization is a two-level MDO algorithm originally developed in 1996 by Braun [1].

CO is expected to maintain expert control in each discipline, incorporate parallel execution by removing iteration loops, and, like BLISS, has a two-level structure similar to industry organizational structures.

To coordinate between disciplines, CO creates copies of all interdisciplinary coupling variables at the system-level. The system optimizer uses these copies to send out design targets to each discipline. Sufficient local degrees of freedom may not exist to satisfy all targets while meeting local constraints; therefore, the local-level subspaces are allowed to depart from the targets, but this departure must be minimized. In theory, if there are enough local-level DOF, variable targets and disciplinary values will converge.

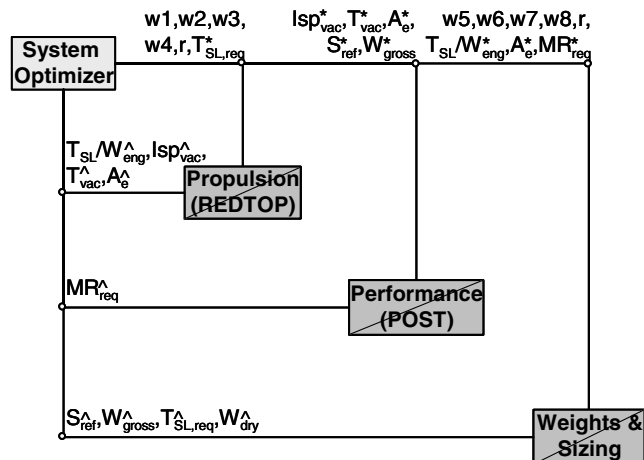


Fig. 5 DSM for BLISS.

Table 5 Final configuration table for BLISS^a

	BLISS-2000 RSM	BLISS-2000 Actual	Units
System objective	W_{dry}	W_{dry}	—
Direction	Minimize	Minimize	—
T_{SL}/W_{eng}	59.52	59.14	—
Isp_{vac}	440.8	441.9	s
c^*	—	7,358	ft/s
Isp_{SL}	—	381.6	s
Cf_{vac}	—	1.892	—
Cf_{SL}	—	1.634	—
T_{SL}/W_{gross}	1.200	1.200	—
ε	52.9	55.6	—
r	7.22	7.22	—
p_c	—	3,100.0	psia
p_e	—	4,999	psia
A_e	275.76	279.91	ft ²
A_t	5.22	5.03	ft ²
SF	1.079	1.079	—
MR	8.03	8.03	—
S_{ref}	4,659	4,659	ft ²
W_{gross}	3,124,072	3,124,062	lb
W_{dry}	305,661	305,660	lb

^aBOLD values represent active constraints.

In CO, as in MCO, the system optimizer sends variable targets to any CAs that deal with the variables as inputs or calculates their actual values as part of its analysis. For example, in the original FPI DSM (Figs. 3 and 4) the variable A_e was an output calculated by propulsion and an input for performance and weights and sizing. In CO, the system sets a target value for A_e . Propulsion optimizes its inputs to match as closely as possible all discipline targets (Isp_{vac} , T_{SL} , etc.), including A_e . Both performance and weights and sizing optimize their input variables (including the local version of A_e) to match their targets.

Local objective (Φ_{Prop} , Φ_{Perf} , and $\Phi_{W\&S}$) functions are formulated to decrease as the local-level optimizer moves closer to meeting targets. Two formulations for reaching this goal were considered:

$$\Phi_{loc} = \sum_{i=1}^{\#targets} \left(1 - \frac{X_i^{loc}}{X_i^t} \right)^2 \quad (12)$$

$$\Phi_{loc} = \sum_{i=1}^{\#targets} \left(\frac{X_i^t - X_i^{loc}}{C_i} \right)^2 \quad (13)$$

Whereas both equations reach a minimum of zero when local values of the design variables (X_i^{loc}) match their targets (X_i^t), their normalization varies. Equation (4) divides X_i^{loc} by X_i^t . In Eq. (5), the difference between X_i^{loc} and X_i^t is calculated and a constant (C_i) is used to normalization purposes. The format used in this study depended on which provided a better local-level convergence for the discipline.

A. CO: Formal Problem Statement

CO has both system and local-level optimization.

1. CO: System Standard Form

The system equality constraint (h) could be separated for each discipline ($\Phi_{loc,i} = 0$) instead of using the single constraint formulation ($\sum \Phi_{loc,i} = 0$). Both formulations are theoretically acceptable. When applied here, the single formulation provided better convergence.

Minimize:

$$\Phi_{sys} \quad W_{dry} \quad (14)$$

Subject to:

$$h \quad \Phi_{Prop} + \Phi_{Perf} + \Phi_{W\&S} = 0 \quad (14a)$$

By Changing:

$$X_{\text{sys}} \quad r^t, \text{Isp}_{\text{vac}}^t, T_{\text{vac}}^t, A_e^t, (T_{\text{SL}}/W_{\text{eng}})^t, S_{\text{ref}}^t, W_{\text{gross}}^t, T_{\text{SL}}^t, \text{MR}^t \quad (14b)$$

2. CO: Propulsion Standard Form

Minimize:

$$\begin{aligned} \Phi_{\text{Prop}} &= \left(\frac{r^t - r^{\text{pp}}}{6} \right)^2 + \left(\frac{T_{\text{SL}}^t - T_{\text{SL}}^{\text{pp}}}{3,500,000} \right)^2 \\ &+ \left(\frac{\text{Isp}_{\text{vac}}^t - \text{Isp}_{\text{vac}}^{\text{pp}}}{400} \right)^2 + \left(\frac{T_{\text{vac}}^t - T_{\text{vac}}^{\text{pp}}}{4,000,000} \right)^2 \\ &+ \left(\frac{A_e^t - A_e^{\text{pp}}}{250} \right)^2 + \left(\frac{T_{\text{SL}}/W_{\text{eng}}^t - T_{\text{SL}}/W_{\text{eng}}^{\text{pp}}}{50} \right)^2 \end{aligned} \quad (15)$$

Subject to:

$$g \quad p_e \geq 5 \text{ psia} \quad (15a)$$

$$\text{Side} \quad 4 \leq r \leq 10$$

$$30 \leq \varepsilon \leq 100$$

$$200 \leq p_c \leq 3100 \text{ psia} \quad (15b)$$

Given as Target:

$$X_{\text{sys}} \quad r^t, \text{Isp}_{\text{vac}}^t, T_{\text{vac}}^t, A_e^t, (T_{\text{SL}}/W_{\text{eng}})^t, T_{\text{SL}}^t \quad (15c)$$

Find:

$$Y_{\text{loc}} \quad \text{Isp}_{\text{vac}}^{\text{pp}}, T_{\text{vac}}^{\text{pp}}, A_e^{\text{pp}}, (T_{\text{SL}}/W_{\text{eng}})^{\text{pp}}, T_{\text{SL}}^{\text{pp}} \quad (15d)$$

By Changing:

$$X_{\text{loc}} \quad r^{\text{pp}}, \varepsilon, p_c, A_t \quad (15e)$$

3. CO: Performance Standard Form

Minimize:

$$\begin{aligned} \Phi_{\text{Perf}} &= \left(1 - \frac{\text{Isp}_{\text{vac}}^{\text{pf}}}{\text{Isp}_{\text{vac}}^t} \right)^2 + \left(1 - \frac{T_{\text{vac}}^{\text{pf}}}{T_{\text{vac}}^t} \right)^2 + \left(1 - \frac{A_e^{\text{pf}}}{A_e^t} \right)^2 \\ &+ \left(1 - \frac{S_{\text{ref}}^{\text{pf}}}{S_{\text{ref}}^t} \right)^2 + \left(1 - \frac{W_{\text{gross}}^{\text{pf}}}{W_{\text{gross}}^t} \right)^2 + \left(1 - \frac{\text{MR}^{\text{pf}}}{\text{MR}^t} \right)^2 \end{aligned} \quad (16)$$

Subject to:

$$\begin{aligned} h \quad h_{\text{insertion}} &= 303,805 \text{ ft} \\ i_{\text{insertion}} &= 51.6 \text{ deg} \\ \gamma_{\text{insertion}} &= 0 \text{ deg} \end{aligned} \quad (16a)$$

Given as Target:

$$X_{\text{sys}} \quad \text{Isp}_{\text{vac}}^t, T_{\text{vac}}^t, A_e^t, S_{\text{ref}}^t, W_{\text{gross}}^t, \text{MR}^t \quad (16b)$$

Find:

$$Y_{\text{loc}} \quad \text{MR}^{\text{pf}} \quad (16c)$$

By Changing:

$$\begin{aligned} X_{\text{loc}} \quad \text{Isp}_{\text{vac}}^{\text{pf}}, T_{\text{vac}}^{\text{pf}}, A_e^{\text{pf}}, S_{\text{ref}}^{\text{pf}}, W_{\text{gross}}^{\text{pf}}, \dot{\theta}_{\text{Azimuth}}, \\ \dot{\theta}_{\text{Pitch1}}, \dot{\theta}_{\text{Pitch2}}, \dot{\theta}_{\text{Pitch3}}, \dot{\theta}_{\text{Pitch4}} \end{aligned} \quad (16d)$$

4. CO: Weights and Sizing Standard Form

Minimize:

$$\begin{aligned} \Phi_{\text{W\&S}} &= \left(1 - \frac{A_e^{\text{ws}}}{A_e^t} \right)^2 + \left(1 - \frac{T_{\text{SL}}/W_{\text{eng}}^{\text{ws}}}{T_{\text{SL}}/W_{\text{eng}}^t} \right)^2 \\ &+ \left(1 - \frac{r^{\text{ws}}}{r^t} \right)^2 + \left(1 - \frac{S_{\text{ref}}^{\text{ws}}}{S_{\text{ref}}^t} \right)^2 + \left(1 - \frac{W_{\text{gross}}^{\text{ws}}}{W_{\text{gross}}^t} \right)^2 \\ &+ \left(1 - \frac{T_{\text{SL}}^{\text{ws}}}{T_{\text{SL}}^t} \right)^2 + \left(1 - \frac{\text{MR}^{\text{ws}}}{\text{MR}^t} \right)^2 \end{aligned} \quad (17)$$

Subject to:

$$\text{Side} \quad T_{\text{SL}}/W_{\text{gross}} \geq 1.2 \quad (17a)$$

Given as Target:

$$X_{\text{sys}} \quad r^t, A_e^t, (T_{\text{SL}}/W_{\text{eng}})^t, S_{\text{ref}}^t, W_{\text{gross}}^t, T_{\text{SL}}^t, \text{MR}^t \quad (17b)$$

Find:

$$Y_{\text{loc}} \quad S_{\text{ref}}^{\text{ws}}, W_{\text{gross}}^{\text{ws}}, T_{\text{SL}}^{\text{ws}}, \text{MR}^{\text{ws}} \quad (17c)$$

By Changing:

$$X_{\text{loc}} \quad r^{\text{ws}}, A_e^{\text{ws}}, T_{\text{SL}}/W_{\text{eng}}^{\text{ws}}, \text{SF}, T_{\text{SL}}/W_{\text{gross}} \quad (17d)$$

B. CO: Data Flow

The DSM for CO is shown in Fig. 6.

C. CO: Results

Observe in Table 6 that the MDO solution obtained by applying CO does not activate constraints for p_c and p_e ; this contrasts solutions derived with AAO and BLISS. Additionally the value of the global objective obtained using CO, $W_{\text{dry}} \approx 303.6$ klb, is lower than determined by both AAO and BLISS, $W_{\text{dry}} \approx 305.5$ klb. One might think that CO did a better job than the previous two, but this lower value is due to large convergence error in the CO model as discussed in Sec. X, “Cross-Technique Configuration Results.” Still, the differences between the values produced for W_{dry} in CO, BLISS, and AAO are low ($<1\%$). Thus, CO seems to agree with AAO, but the larger error produced with this methodology makes it uncertain.

CO produced a 4.39% reduction in W_{dry} versus the best FPI result and a 3.60% reduction in W_{gross} .

IX. Modified Collaborative Optimization

Modified Collaborative Optimization is a MDO algorithm developed in 1998 by DeMiguel and Murray [2].

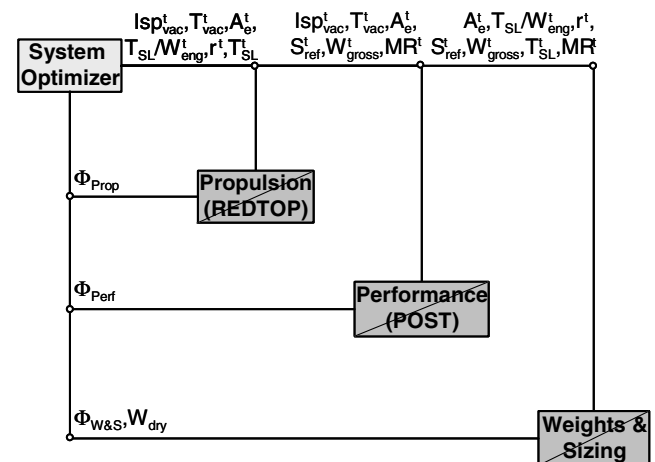


Fig. 6 DSM for CO and MCO.

Table 6 Final configuration table for CO^a

	CO	Units
System objective	W_{dry}	—
Direction	Minimize	—
$T_{\text{SL}}/W_{\text{eng}}$	59.34	—
Isp_{vac}	440.8	s
c^*	7,334	ft/s
Isp_{SL}	380.5	s
Cf_{vac}	1.892	—
Cf_{SL}	1.633	—
$T_{\text{SL}}/W_{\text{gross}}$	1.200	—
ε	54.6	—
r	7.31	—
p_c	3,036.2	psia
p_e	5.077	psia
A_e	280.06	ft ²
A_t	5.13	ft ²
SF	1.075	—
MR	7.96	—
S_{ref}	4,624	ft ²
W_{gross}	3,097,190	lbf
W_{dry}	303,663	lbf

^aBOLD values represent active constraints.

MCO is a derivative of CO attempting to “surmount some deep technical challenges” [2] present in the formulation of CO. The developers of MCO noted deficiencies in the lack of a proof of convergence and gradient optimization difficulties due to a vanishing gradient effect as the local objectives approach their minimums. MCO’s architecture is similar to that of CO with the same inputs and outputs entering and leaving the CAs.

The first change is that MCO uses an “exact” [2] penalty function as the system-level objective. MCO uses the local-level objective functions as penalty terms for the system objective function, creating an unconstrained system-level problem. This contrasts CO, which imposed constraints at the system-level to enforce that local-level objective functions reach their expected minimums at zero.

Furthermore, MCO does away with the quadratic form of the local objectives and replaces it with a format similar to linear programming called individual discipline feasible (IDF). As in CO, the system may call for an infeasible set of targets where local disciplines cannot match given targets. IDF solves this by introducing additional local-level variables and constraints. In IDF, if the set of targets is infeasible, elastic variables (s and t) are added to correct differences between local-level values and given targets. The local objective is now to minimize the amount of corrections to be performed using elastic variables. All variables in IDF are required to have positive values; thus, elastic variables must be introduced for both when the local variable is less than (s) or greater than (t) the target value. IDF only allows equality constraints; thus, local-level inequality constraints are changed to equality constraints by adding another elastic variable.

A. MCO: Formal Problem Statement

MCO has both system and local-level optimization.

1. MCO: System Standard Form

In the next equation, r_p is a penalty parameter used to alter the acceptable level of error in the penalty function.

Minimize:

$$\Phi_{\text{sys}} = W_{\text{dry}} + r_p^*(\Phi_{\text{Prop}} + \Phi_{\text{Perf}} + \Phi_{\text{W\&S}}) \quad (18)$$

Subject to:

By Changing:

$$X_{\text{sys}} = r^t, \text{Isp}_{\text{vac}}^t, T_{\text{vac}}^t, A_e^t, T_{\text{SL}}/W_{\text{eng}}^t, S_{\text{ref}}^t, W_{\text{gross}}^t, T_{\text{SL}}^t, \text{MR}^t \quad (18a)$$

2. MCO: Propulsion Standard Form

Minimize:

$$\Phi_{\text{Prop}} = (s_r + t_r) + (s_{\text{Isp}_{\text{vac}}} + t_{\text{Isp}_{\text{vac}}}) + (s_{T_{\text{vac}}} + t_{T_{\text{vac}}}) + (s_{A_e} + t_{A_e}) + (s_{T_{\text{vac}}/W_{\text{eng}}} + t_{T_{\text{vac}}/W_{\text{eng}}}) + (s_{T_{\text{SL}}} + t_{T_{\text{SL}}}) \quad (18b)$$

Subject to:

$$\begin{aligned} h \quad p_e^{\text{pp}} - s_{p_e} - 5 \text{ psia} &= 0 \\ r^{\text{pp}} + s_r - t_r &= r^t \\ \text{Isp}_{\text{vac}}^{\text{pp}} + s_{\text{Isp}_{\text{vac}}} - t_{\text{Isp}_{\text{vac}}} &= \text{Isp}_{\text{vac}}^t \\ T_{\text{vac}}^{\text{pp}} + s_{T_{\text{vac}}} - t_{T_{\text{vac}}} &= T_{\text{vac}}^t \\ A_e^{\text{pp}} + s_{A_e} - t_{A_e} &= A_e^t \\ (T_{\text{SL}}/W_{\text{eng}})^{\text{pp}} + s_{T_{\text{SL}}/W_{\text{eng}}} - t_{T_{\text{SL}}/W_{\text{eng}}} &= (T_{\text{SL}}/W_{\text{eng}})^t \\ T_{\text{SL}}^{\text{pp}} + s_{T_{\text{SL}}} - t_{T_{\text{SL}}} &= T_{\text{SL}}^t \end{aligned} \quad (18c)$$

$$\text{Side} \quad 4 \leq r \leq 10 \quad 30 \leq \varepsilon \leq 100 \quad 200 \leq p_c \leq 3100 \text{ psia}$$

$$\begin{aligned} s_{p_e}, s_r, t_r, s_{\text{Isp}_{\text{vac}}}, t_{\text{Isp}_{\text{vac}}}, s_{T_{\text{vac}}}, t_{T_{\text{vac}}}, s_{A_e}, t_{A_e}, s_{T_{\text{SL}}/W_{\text{eng}}}, \\ t_{T_{\text{SL}}/W_{\text{eng}}}, s_{T_{\text{SL}}}, t_{T_{\text{SL}}} \geq 0 \end{aligned} \quad (18d)$$

Given as Target:

$$X_{\text{sys}} = r^t, \text{Isp}_{\text{vac}}^t, T_{\text{vac}}^t, A_e^t, (T_{\text{SL}}/W_{\text{eng}})^t, T_{\text{SL}}^t \quad (18e)$$

Find:

$$Y_{\text{loc}} = \text{Isp}_{\text{vac}}^{\text{pp}}, T_{\text{vac}}^{\text{pp}}, A_e^{\text{pp}}, (T_{\text{SL}}/W_{\text{eng}})^{\text{pp}}, T_{\text{SL}}^{\text{pp}} \quad (18f)$$

By Changing:

$$\begin{aligned} X_{\text{loc}} = r^{\text{pp}}, \varepsilon, c, A_t, s_{p_e}, s_r, t_r, s_{\text{Isp}_{\text{vac}}}, t_{\text{Isp}_{\text{vac}}}, s_{T_{\text{vac}}}, t_{T_{\text{vac}}}, s_{A_e}, t_{A_e}, \\ s_{T_{\text{SL}}/W_{\text{eng}}}, t_{T_{\text{SL}}/W_{\text{eng}}}, s_{T_{\text{SL}}}, t_{T_{\text{SL}}} \end{aligned} \quad (18g)$$

3. MCO: Performance Standard Form

Minimize:

$$\Phi_{\text{Perf}} = (s_{\text{Isp}_{\text{vac}}} + t_{\text{Isp}_{\text{vac}}}) + (s_{T_{\text{vac}}} + t_{T_{\text{vac}}}) + (s_{A_e} + t_{A_e}) + (s_{S_{\text{ref}}} + t_{S_{\text{ref}}}) + (s_{W_{\text{gross}}} + t_{W_{\text{gross}}}) + (s_{\text{MR}} + t_{\text{MR}}) \quad (19)$$

Subject to:

$$\begin{aligned} h \quad h_{\text{insertion}} &= 303,805 \text{ ft} \\ i_{\text{insertion}} &= 51.6 \text{ deg} \\ \gamma_{\text{insertion}} &= 0 \text{ deg} \\ \text{Isp}_{\text{vac}}^{\text{pf}} + s_{\text{Isp}_{\text{vac}}} - t_{\text{Isp}_{\text{vac}}} &= \text{Isp}_{\text{vac}}^t \\ T_{\text{vac}}^{\text{pf}} + s_{T_{\text{vac}}} - t_{T_{\text{vac}}} &= T_{\text{vac}}^t \\ A_e^{\text{pf}} + s_{A_e} - t_{A_e} &= A_e^t \\ S_{\text{ref}}^{\text{pf}} + s_{S_{\text{ref}}} - t_{S_{\text{ref}}} &= S_{\text{ref}}^t \\ W_{\text{gross}}^{\text{pf}} + s_{W_{\text{gross}}} - t_{W_{\text{gross}}} &= W_{\text{gross}}^t \\ \text{MR}^{\text{pf}} + s_{\text{MR}} - t_{\text{MR}} &= \text{MR}^t \\ s_{\text{Isp}_{\text{vac}}}, t_{\text{Isp}_{\text{vac}}}, s_{T_{\text{vac}}}, t_{T_{\text{vac}}}, s_{A_e}, t_{A_e}, s_{S_{\text{ref}}}, t_{S_{\text{ref}}}, s_{W_{\text{gross}}}, \\ t_{W_{\text{gross}}}, s_{\text{MR}}, t_{\text{MR}} &\geq 0 \end{aligned} \quad (19a)$$

Given as Target:

$$X_{\text{sys}} \quad \text{Isp}_{\text{vac}}^t, T_{\text{vac}}^t, A_e^t, S_{\text{ref}}^t, W_{\text{gross}}^t, \text{MR}^t \quad (19b)$$

Find:

$$Y_{\text{loc}} \quad \text{MR}^{\text{pf}} \quad (19c)$$

By Changing:

$$X_{\text{loc}} \quad \text{Isp}_{\text{vac}}^{\text{pf}}, T_{\text{vac}}^{\text{pf}}, A_e^{\text{pf}}, S_{\text{ref}}^{\text{pf}}, W_{\text{gross}}^{\text{pf}}, \dot{\theta}_{\text{Azimuth}}, \dot{\theta}_{\text{Pitch1}}, \dot{\theta}_{\text{Pitch2}}, \dot{\theta}_{\text{Pitch3}}, \dot{\theta}_{\text{Pitch4}}, s_{\text{Isp}_{\text{vac}}}, t_{\text{Isp}_{\text{vac}}}, s_{T_{\text{vac}}}, t_{T_{\text{vac}}}, s_{A_e}, t_{A_e}, s_{S_{\text{ref}}}, t_{S_{\text{ref}}}, s_{W_{\text{gross}}}, t_{W_{\text{gross}}}, s_{\text{MR}}, t_{\text{MR}} \quad (19d)$$

4. MCO: Weights and Sizing Standard Form

Minimize:

$$\begin{aligned} \Phi_{\text{W\&S}} & (s_{A_e} + t_{A_e}) + (s_{T_{\text{SL}}/W_{\text{eng}}} + t_{T_{\text{SL}}/W_{\text{eng}}}) \\ & + (s_r + t_r) + (s_{S_{\text{ref}}} + t_{S_{\text{ref}}}) + (s_{W_{\text{gross}}} + t_{W_{\text{gross}}}) \\ & + (s_{T_{\text{SL}}} + t_{T_{\text{SL}}}) + (s_{\text{MR}} + t_{\text{MR}}) \end{aligned} \quad (20)$$

Subject to:

$$\begin{aligned} h \quad & (T_{\text{SL}}/W_{\text{eng}})^{\text{ws}} + s_{T_{\text{SL}}/W_{\text{eng}}} - t_{T_{\text{SL}}/W_{\text{eng}}} = (T_{\text{SL}}/W_{\text{eng}})^t \\ & A_e^{\text{ws}} + s_{A_e} - t_{A_e} = A_e^t \\ & r^{\text{ws}} + s_r - t_r = r^t \\ & S_{\text{ref}}^{\text{ws}} + s_{S_{\text{ref}}} - t_{S_{\text{ref}}} = S_{\text{ref}}^t \\ & W_{\text{gross}}^{\text{ws}} + s_{W_{\text{gross}}} - t_{W_{\text{gross}}} = W_{\text{gross}}^t \\ & T_{\text{SL}}^{\text{ws}} + s_{T_{\text{SL}}} - t_{T_{\text{SL}}} = T_{\text{SL}}^t \\ & \text{MR}^{\text{ws}} + s_{\text{MR}} - t_{\text{MR}} = \text{MR}^t \end{aligned} \quad (20a)$$

Side $T_{\text{SL}}/W_{\text{gross}} \geq 1.2$

$$\begin{aligned} & s_{A_e}, t_{A_e}, s_{T_{\text{SL}}/W_{\text{eng}}}, s_r, t_r, s_{S_{\text{ref}}}, t_{S_{\text{ref}}}, s_{W_{\text{gross}}}, t_{W_{\text{gross}}}, \\ & s_{T_{\text{SL}}}, t_{T_{\text{SL}}}, s_{\text{MR}}, t_{\text{MR}} \geq 0 \end{aligned} \quad (20b)$$

Given as Target:

$$X_{\text{sys}} \quad r^t, A_e^t, (T_{\text{SL}}/W_{\text{eng}})^t, S_{\text{ref}}^t, W_{\text{gross}}^t, T_{\text{SL}}^t, \text{MR}^t \quad (20c)$$

Find:

$$Y_{\text{loc}} \quad S_{\text{ref}}^{\text{ws}}, W_{\text{gross}}^{\text{ws}}, T_{\text{SL}}^{\text{ws}}, \text{MR}^{\text{ws}} \quad (20d)$$

By Changing:

$$\begin{aligned} X_{\text{loc}} \quad & r^{\text{ws}}, A_e^{\text{ws}}, (T_{\text{SL}}/W_{\text{eng}})^{\text{ws}}, \text{SF}, T_{\text{SL}}/W_{\text{gross}}, s_{A_e}, t_{A_e}, \\ & s_{T_{\text{SL}}/W_{\text{eng}}}, t_{T_{\text{SL}}/W_{\text{eng}}}, s_r, t_r, s_{S_{\text{ref}}}, t_{S_{\text{ref}}}, s_{W_{\text{gross}}}, t_{W_{\text{gross}}}, s_{T_{\text{SL}}}, \\ & t_{T_{\text{SL}}}, s_{\text{MR}}, t_{\text{MR}} \end{aligned} \quad (20e)$$

B. MCO: Data Flow

The DSM for MCO is identical to that of CO shown in Fig. 6.

C. MCO: Results

The main differences between CO and MCO are that MCO uses IDF for the local objective function and removes equality constraints at the system level, replacing them with a penalty function. Whereas IDF seemed to offer some advantages when applied, the penalty function formulation led to inconsistent results. The resulting MDO solution varied greatly with the value of the penalty parameter (r_p); see Fig. 7, an unexpected and undesirable phenomenon.

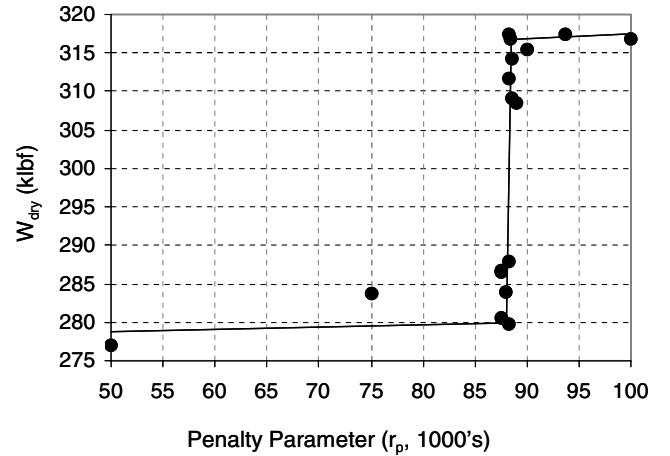


Fig. 7 Resultant W_{dry} vs penalty parameter (r_p).

As can be observed in Fig. 7, the resulting value for W_{dry} using MCO had a step function relation with r_p . If r_p were too large, then the MCO model could not improve its initialization point (the best FPI configuration, $W_{\text{dry}} \approx 317$ klbf) and the optimizer would not move. If r_p were too small, then the MCO configuration would move from its initial point and drive the value of W_{dry} down to around $W_{\text{dry}} \approx 285$ klbf. These low results had very poor convergence with errors often above 5%.

The value of W_{dry} jumps at $88,000 \leq r_p \leq 90,000$. It was impossible to isolate a value of r_p that produced a W_{dry} similar to the value found using AAO and BLISS ($W_{\text{dry}} \approx 305$ klbf), as there was not a smooth relationship. In addition, two identical MCO trials could produce drastically different results. If a trial run produced a W_{dry} value approaching expectations from BLISS and AAO, when that trial was retried, the optimizer often never moved or fell to the $W_{\text{dry}} \approx 285$ klbf range.

The resultant inconsistencies observed in the MCO model made it impossible to draw any conclusions from the test trials.

X. Cross-Technique Configuration Results

Table 7 shows final configurations derived through the application of each technique. One can observe that the iterative solution (FPI) produced a suboptimal result, with the best FPI configuration producing a resultant W_{dry} about 4% higher than the true optimum ($W_{\text{dry}} \approx 305.5$ klb) found by applying AAO or BLISS.

In Table 7, it appears that CO produced a better result with respect to the global objective. This result is deceptively good due to significant convergence error in the technique. Figure 8, shows box plots [13] of the convergence errors in the coupling variables used in each technique. CO has a much larger convergence error than any other technique successfully applied in this study. This is due to local

Table 7 Final configuration table, all techniques^a

	Iterative	AAO	BLISS	CO	Units
Isp _{vac}	443.1	440.1	441.99	440.8	s
Isp _{SL}	383.8	378.4	381.6	380.5	s
Cf _{vac}	1.884	1.902	1.892	1.892	—
Cf _{SL}	1.631	1.635	1.634	1.633	—
$T_{\text{SL}}/W_{\text{gross}}$	1.20	1.200	1.200	1.200	—
ε	54.3	57.5	55.6	54.6	—
r	7.00	7.51	7.22	7.31	—
p_c	3,100.0	3,100.0	3,100.0	3,036.2	psia
p_e	5.003	4.999	4.999	5.077	psia
A_e	281.56	290.13	279.91	280.06	ft ²
MR	7.96	8.07	8.03	7.96	—
S_{ref}	4,801	4,610	4,659	4,624	ft ²
W_{gross}	3,213	3,139	3,124	3,097	klbf
W_{dry}	317.6	305.1	305.7	303.7	klbf

^aBOLD values represent active constraints.

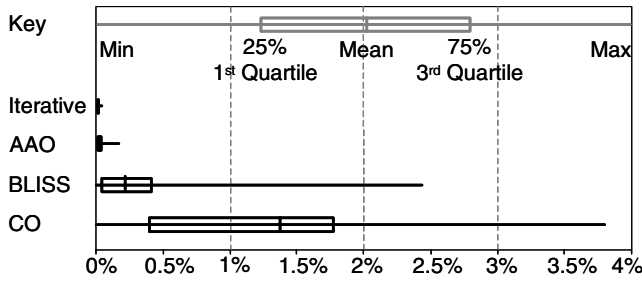


Fig. 8 Convergence error box plots, all techniques.

optimizers having difficulty matching given targets and the discipline error versus the target being independent for each discipline.

CO's discipline error independence is what creates artificially optimistic results. The system optimizer takes advantage that local optimizers can have different errors for given targets and chooses the most opportune error directions, benefiting the system goal of minimizing W_{dry} . An example of this "opportune error direction effect" is shown in Fig. 9.

Isp_{vac} is calculated by propulsion and used by performance to perform trajectory analysis. The system optimizer sends out a target value for Isp_{vac} (440 in the example). Because of the vanishing gradient effect, numerical errors, etc., there will be a convergence error between the system target and the value used by the local discipline. This system-discipline error is only 0.9% for propulsion, $(440 - 436)/440$, and 1.1% for performance, $(445 - 440)/440$. Because local convergence error is inevitable, the system optimizer takes advantage of it. It chooses the most opportune error directions to help minimize W_{dry} . Therefore, propulsion will actually arrive at an Isp below its target value and performance above its target value, and the two disciplines will have a larger convergence error between them (2%) than their individual error versus the target. The percent errors and directions observed with respect to their desired targets for the CO configuration are shown in Fig. 10.

XI. Analysis and Discussions

Analysis and discussions of the results presented were drawn for this study's three objectives as listed at the beginning of this paper.

A. Benefits of MDO vs FPI

Results presented show that RLV optimization employing MDO techniques offers some improvement over results obtained using the FPI process. This confirms that, without human intervention, the traditional method using FPI does not provide optimum results. Whereas use of MDO showed a modest improvement in the global objective, this benefit may increase for large, complex problems for which MDO methods are designed.

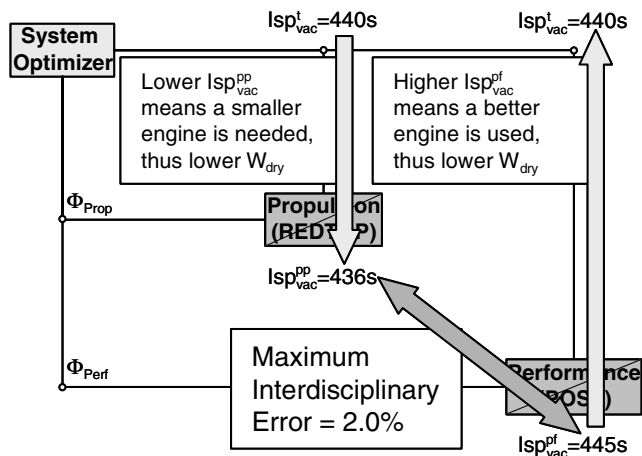


Fig. 9 Example of opportune error direction effect, Isp_{vac} .

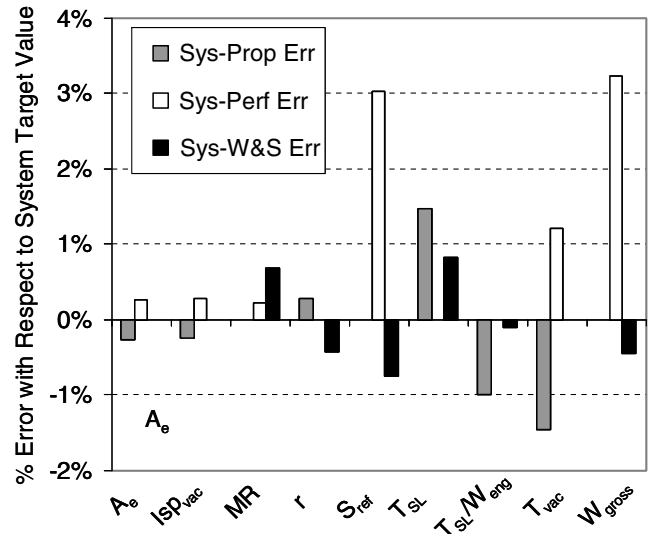


Fig. 10 Percent error and direction with respect to system targets for CO configuration.

The application of MDO resulted in a vehicle dry weight (W_{dry}) reduction of about 4% versus the best FPI solution and 14% below the industry standard FPI configuration. If the size of the MDO problem to be solved is small and the execution of the CAs involved is not very costly, then traditional methods using FPI will probably be the best choice. For large problems with time-consuming CAs, the implementation cost of MDO will more likely be offset by its benefits.

For problems with a high dimensionality coupling between CAs, it is unclear if MDO techniques will be practicable. Bi-level MDO methods like BLISS-2000, CO, and MCO may prove unfeasible as they add new system-level variables that may complicate the problem beyond the ability of the system-level optimizer. AAO may be feasible if the underlying analyses for the CAs have very predictable behaviors, allowing accurate and reproducible gradients to be calculated. However, real-world aerospace system design problems tend to have low dimensionality coupling. The traditional use of FPI in the aerospace industry has led to design disciplines with a minimum number of interdisciplinary design variables in order to reduce the number of iterations needed to converge a system.

B. Authenticity of Test Problem

The selection of a test problem was limited to those for which AAO might still be applicable to validate newer multilevel MDO techniques. The test problem used for this study seemed to border the size and complexity still solvable using AAO.

Despite size restrictions, the RLV test problem selected had characteristics increasing its likeness to "real-world" problems:

- 1) Disciplines were broken down along the conventional disciplinary lines.
- 2) Technology reduction factors were added to more accurately model the technologies to be used in a next-generation vehicle.
- 3) The base vehicle is a real concept studied by both NASA and industry.
- 4) Widely used legacy codes or similar were used for the design and analysis of each discipline.

C. Comparison Between CO, MCO, and BLISS

It was known that this study would be unable to conclude if any one MDO technique is more promising than the others, as it is but one study from which it is impossible to draw any statistically significant conclusions. Conversely, this study was successful in using the blocking effect to reduce the number of external factors making it difficult to determine variance between the multilevel MDO techniques.

Table 8 Execution time, all techniques

	Iteration	AAO	BLISS	CO
Total execution time (no parallel execution)	5–20 min	40–50 min	2–3 h	3–4 h
Estimated execution time (with parallel processing)	N/A	N/A	10–20 min	1–2 h

Table 9 Qualitative report card, all techniques

Criteria	Credits	Iteration	AAO	BLISS	CO	MCO
Implementation difficulty	3	A	C	B+	C+	Incomplete
Total execution Time	3	A	A–	B+	B–	C
Model robustness	3	A	D	B+	B	Incomplete
Formulation difficulty	2	A	A	B+	B–	C–
Optimization deftness	4	D	A–	A	B	Incomplete
Convergence error	3	A	A–	B+	C+	B
GPA		3.11	3.00	3.46	2.68	Incomplete

For FPI and each MDO method successfully applied (AAO, BLISS-2000, and CO) the total execution wall time needed to solve the RLV MDO problem was measured, as shown in Table 8. Although parallel processing was not available for this study, an estimate of the total wall time should parallel processing be implemented is also provided. A time range value is provided as the total execution time varies with different initialization points.

Drawing on the experience of performing multiple applications of different MDO techniques on the same problem, Table 9 shows a qualitative report card where each technique received a grade point average (GPA). Higher GPAs indicate better performance. The left column shows qualitative criteria for which each MDO technique received a grade and the “Credits” column shows the importance given to each criteria. The more credits the more importance the criterion is when calculating GPA. Grades are only accurate with relation to each other for this specific study.

Although a model of the next-generation RLV was created for each multilevel MDO technique selected at the start of the study, the MCO model was never able to reach enough behavioral consistency for any conclusions to be made, thus there is no GPA given.

From Table 8, one can see that the BLISS algorithm was the best performer in this study, as it allowed MDO to be employed while making few changes to original legacy codes created with FPI in mind.

XII. Conclusions

This study had three main objectives: to determine the benefits of multidisciplinary optimization versus designs produced using fixed-point iteration, to create a test problem realistic enough to enable the evaluation of MDO techniques, and to perform a qualitative and quantitative comparison of several novel MDO techniques. The results showed that employing MDO techniques exhibited some improvement over designs obtained by using FPI, the reusable launch vehicle test problem selected was suitable for the study of MDO techniques, and the novel MDO techniques were successfully compared, with the BLISS-2000 algorithm showing the best overall performance.

Although BLISS-2000 was the multilevel MDO technique that exhibited the most promise to be practicably applied to large, real-world optimization problems, this study is only one data point. It is statistically impossible to declare BLISS “most promising” unless more studies employing the blocking effect substantiate the results found here.

Acknowledgments

This work was funded by the University Research, Engineering, and Technology Institute (URETI) Program. Sponsorship for N. F. Brown was provided by the Northrop Grumman Corporation, Mission Systems. N. F. Brown and J. R. Olds would like to thank Jaroslaw Sobieski of NASA Langley, Robert Braun, Tim Kokan, and all of the members of the Space Systems Design Lab (SSDL) at the Georgia Institute of Technology.

References

- [1] Braun, R. D., “Collaborative Architecture for Large-Scale Distributed Design,” Ph.D. Dissertation, Aeronautics and Astronautics Dept., Stanford Univ., Stanford, CA, 1996.
- [2] DeMiguel, A. V., and Murray, W., “An Analysis of Collaborative Optimization Methods,” AIAA Paper 2000-4720, Sept. 2000.
- [3] Sobieszanski-Sobieski, J., Agte, J., and Sandusky, R., “Bi-Level Integrated System Synthesis,” AIAA Paper 1998-4916, Sept. 1998.
- [4] Sobieszanski-Sobieski, J., Altus, T., Phillips, M., and Sandusky, R., “Bi-Level Integrated System Synthesis for Concurrent and Distributed Processing,” *AIAA Journal*, Vol. 41, No. 10, 2003, pp. 1996–2003.
- [5] Alexandrov, N. M., “Comparative Properties of Collaborative Optimization and Other Approaches to MDO,” NASA CR-1999-209354, also Institute for Computer Applications in Science and Engineering Report No. 99-24, NASA Langley Research Center, Hampton, VA, July 1999.
- [6] Alexandrov, N. M., and Lewis, R. M., “Analytical and Computational Properties of Distributed Approaches to MDO,” AIAA Paper 2000-4718, Sept. 2000.
- [7] Budianto, I., and Olds, J., “A Collaborative Optimization Approach to Design and Deployment of a Space Based Infrared System Constellation,” Institute of Electrical and Electronics Engineers Paper P335E, March 2000.
- [8] Kroo, I., and Manning, V., “Collaborative Optimization: Status and Directions,” AIAA Paper 2000-4721, Sept. 2000.
- [9] Cormier, T., Scott, A., Ledsinger, L., McCormick, D., Way, D., and Olds, J., “Comparison of Collaborative Optimization to Conventional Design Techniques for a Conceptual RLV,” AIAA Paper 2000-4885, Sept. 2000.
- [10] Perez, R., Liu, H., and Behdinan, K., “Evaluation of Multidisciplinary Optimization Approaches for Aircraft Conceptual Design,” AIAA Paper 2004-4537, Aug. 2004.
- [11] Kodiyalam, S., “Evaluation of Methods for Multidisciplinary Design Optimization (MDO), Phase 1,” NASA CR-1998-208716, Sept. 1998.
- [12] Kodiyalam, S., and Yuan, C., “Evaluation of Methods for Multidisciplinary Design Optimization (MDO), Part 2,” NASA CR-2000-210313, Nov. 2000.
- [13] Hayter, A. J., *Probability and Statistics for Engineers and Scientists*, 2nd ed., Duxbury Thompson Learning, Pacific Grove, CA, 2002.
- [14] Isakowitz, S. J., Hopkins, J. P., and Hopkins, J. B., *International Reference Guide to Space Launch Systems*, 3rd ed., AIAA, Reston, VA, 1999.
- [15] Olds, J., Crocker, A., Bradford, J., and Charania, A. C., “Concept Overview and Model Operation: Reduced Order Simulation for Evaluating Technologies and Transport Architectures (ROSETTA),” SpaceWorks Engineering, Atlanta, GA.
- [16] MacConochie, I. O., “Characterization of Subsystems for a WB-003 Single Stage Shuttle,” NASA CR-2002-211249, 2002.
- [17] REDTOP, Rocket Engine Design Tool for Optimal Performance, Release 2, SpaceWorks Engineering, Atlanta, GA, 2004.
- [18] Way, D. W., and Olds, J. R., “SCORES: Web-Based Rocket Propulsion Analysis Tool for Space Transportation System Design,” AIAA Paper 99-2353, June 1999.
- [19] Powell, R. W., Striepe, A., Desai, P. N., Braun, R. D., Brauer, G. L., Cornick, D. E., Olson, D. W., Petersen, F. M., and Stevenson, R., Program to Optimize Simulated Trajectories (POST): Vol. 2 Utilization Manual Version 5.2, Oct. 1997.
- [20] ModelCenter, Ver. 5.0.1, Phoenix Integration, Blacksburg, VA, 2003.
- [21] Vanderplaats, G. N., *Numerical Optimization Techniques for Engineering and Design*, 3rd ed., Vanderplaats Research & Development, Colorado Springs, CO, 1999.
- [22] ProbWorks: ModelCenter, Pi Blue Software, Atlanta, GA, 2004.